JOURNAL OF CHEMICAL INFORMATION AND MODELING

Article

pubs.acs.org/jcim

Analyzing the Molecular Basis of Enzyme Stability in Ethanol/Water Mixtures Using Molecular Dynamics Simulations

Diana Lousa, António M. Baptista, and Cláudio M. Soares*

Instituto de Tecnologia Química e Biológica, Universidade Nova de Lisboa, Av. da República, 2780-157 Oeiras, Portugal

Supporting Information

ABSTRACT: One of the drawbacks of nonaqueous enzymology is the fact that enzymes tend to be less stable in organic solvents than in water. There are, however, some enzymes that display very high stabilities in nonaqueous media. In order to take full advantage of the use of nonaqueous solvents in enzyme catalysis, it is essential to elucidate the molecular basis of enzyme stability in these media. Toward this end, we performed μs-long molecular dynamics simulations using two homologous proteases, pseudolysin, and thermolysin, which are known to have considerably different stabilities in solutions containing ethanol.[1] The analysis of the simulations indicates that pseudolysin is more stable than thermolysin in ethanol/water mixtures and that the disulfide bridge between C30 and C58 is important for the stability of the former enzyme, which is consistent with previous experimental observations.[1,2] Our results indicate that thermolysin has a higher tendency to interact with ethanol molecules (especially through van der Waals contacts) than pseudolysin, which can lead to the disruption of intraprotein hydrophobic interactions and ultimately result in protein unfolding. In the absence of the C30−C58 disulfide bridge, pseudolysin undergoes larger conformational changes, becoming more open and more permeable to ethanol molecules which accumulate in its interior and form hydrophobic interactions with the enzyme, destroying its structure. Our observations are not only in good agreement with several previous experimental findings on the stability of the enzymes studied in ethanol/water mixtures but also give an insight on the molecular determinants of this stability. Our findings may, therefore, be useful in the rational development of enzymes with increased stability in these media.

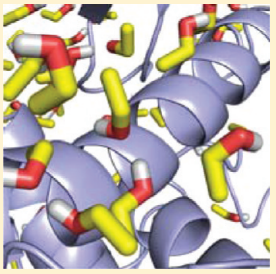

INTRODUCTION

The application of organic solvents in enzyme catalysis is of great technological and fundamental interest, because enzymes in these media can display novel properties,[3] such as the capacity to catalyze reactions that are not feasible in water,[4] different substrate specificity and enantioselectivity,[5−9] and molecular memory.[10−13] Computational tools for the understanding of enzyme mechanisms, both at the kinetic level (see refs 14−17 for recent examples) as well as at the atomic level,[9,13,18−22] have proven to be important for a deeper understanding of enzyme catalysis[23−26] and, in particular, enzyme catalysis in nonaqueous solvents.[27,28]

Despite its great technological potential, the use of enzymes in nonaqueous solvents has limitations, and one of the most serious is the fact that enzymes in organic solvents are usually less stable than in water. Several strategies have been used to overcome this limitation, including chemical modification, enzyme immobilization, protein engineering, and directed evolution.[29,30] Another promising approach is the search for enzymes that are naturally stable in organic solvents.[31,32] Using the latter strategy, Ogino et al. found that the stability of the protease pseudolysin (PSL) in solutions containing hydrophilic solvents is higher than in pure water.[1] Moreover, they observed that pseudolysin is more stable in these solutions than other proteases, namely subtilisin Carlsberg, α-chymotrypsin, and thermolysin (TLN).[1]

Pseudolysin, also known as *Pseudomonas elastase*, is a zinc metalloprotease secreted by *Pseudomonas aeruginosa* that belongs to the protein family M4. Although its precise biological function is not completely clear, it is known that this enzyme plays a role in the infectious process of *P. aeruginosa*[33−35] and that PSL can degrade elastin (hence the name elastase)[36] as well as collagen,[37] human IgG,[38] and other important human proteins and peptides. Thermolysin is a thermostable enzyme secreted by *Bacillus thermoproteolyticus*. This protease is the prototypical enzyme of the M4 family of zinc metalloproteases, being a neutral endopeptidase that specifically hydrolyzes peptide bonds containing hydrophobic residues.[39] The different stability displayed by pseudolysin and thermolysin in ethanol/water mixtures is curious, given that they share 28% sequence identity, a similar fold, and a conserved catalytic center (composed by a zinc atom tetrahedrally coordinated by a glutamate, two histidines, and a water molecule). The main difference between the structures of the two proteases is the presence of two disulfide bonds in pseudolysin (between Cys-30 and Cys-58 and between Cys-270 and Cys-297) that are absent from thermolysin (see Figure 1). It has been shown that the disulfide bond located in the C-terminal domain is essential for the protein activity, whereas the bond between Cys-30 and Cys-58 is very important for the solvent stability of PSL.[2]

Our aim is to gain a deeper understanding of the molecular determinants underlying the different stability displayed by

Received: September 23, 2011
Published: January 16, 2012

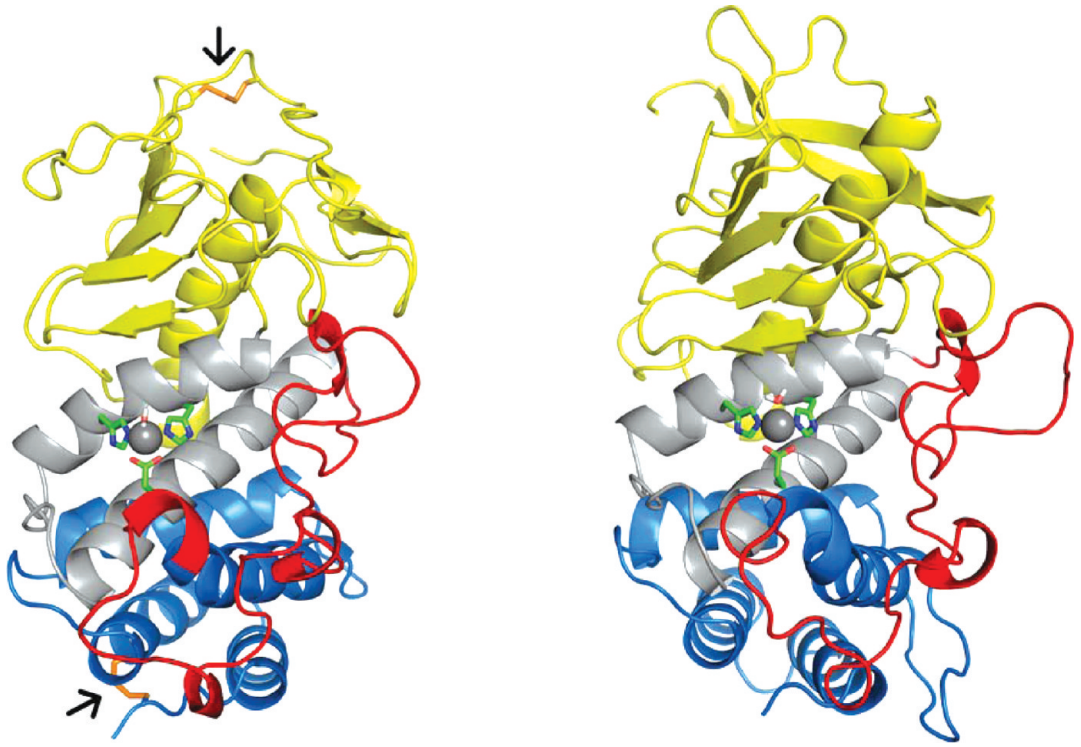

Figure 1. X-ray structures of pseudolysin (left) and thermolysin (right). Both proteins are composed by three domains: N-terminal domain (yellow), active site domain (gray), and C-terminal domain (blue and red). The red color is used to highlight the loop comprising residues 180−224 and 181−229 in PSL and TLN, respectively, that is very mobile (see the Results Section). The residues of the catalytic center are shown in sticks, and the two arrows indicate the disulfide bridges of PSL, which are displayed using orange sticks.

pseudolysin and thermolysin in solutions containing ethanol. Additionally, we intend to elucidate the role played by the disulfide bond between C-30 and C-58 in maintaining the stability of pseudolysin. With this objective, we have performed μs-long molecular dynamics (MD) simulations of PSL and TLN, in pure water and in an ethanol/water mixture, and of the C58G mutant of PSL, in ethanol/water. The behavior of the enzymes in our simulations is consistent with the previous experimental observations,[1,2] and the analysis of the protein−ethanol interactions enabled us to unravel the molecular causes of this behavior.

MATERIALS AND METHODS

For thermolysin, the X-ray structure determined by Holland et al. at 1.70 Å resolution (PDB code: 1LNF)[40] was used. In the pseudolysin simulations, we used the X-ray structure obtained by Thayer et al. at 1.50 Å resolution (PDB code: 1EZM).[41] The mutant C58G of pseudolysin was obtained by removing all the side-chain atoms of Cys-58, transforming this residue into a glycine.

The determination of the protonation state of each titrable site in the protein at pH 7 was performed using a methodology developed by us, based on continuum electrostatics and Monte Carlo sampling of protonation states, that has been explained in detail before[42,43] (further details can be found in the Supporting Information).

We performed five sets of MD simulations, as summarized in Table 1. Given that we are trying to capture a slow phenomenon, i.e., loss of protein stability, the simulations were run for 1 μs. Although 1 μs is a short period of time compared with the time scale of unfolding, our aim was to capture early signs of stability. Additionally, in order to obtain a good sampling, five replicates were calculated for each system under study.

Table 1. Description of the Systems Analyzed in This Work

short description	enzyme	solvent
PSL in water	wild-type pseudolysin	water
PSL in eth/water	wild-type pseudolysin	ethanol + water (25% v/v)
PSL-C58G in eth/water	C58G mutant of pseudolysin	Ethanol + water (25% v/v)
TLN in water	wild-type thermolysin	water
TLN in eth/water	wild-type thermolysin	ethanol + water (25% v/v)

MD simulations were performed with the GROMACS package,[44] version 4.0,[45] using the GROMOS 53A6 force field.[46] Water was modeled with the simple point charge (SPC)[47] model. Bond lengths of the solute and ethanol molecules were constrained with LINCS,[48] and for water molecules, the SETTLE[49] algorithm was used. The temperature and pressure were kept constant during the simulations. Temperature coupling was done using the Berendsen thermostat[50] with a temperature coupling constant of 0.1 ps and a reference temperature of 300 K. The protein and solvent (water or ethanol/water) were coupled to separate heat baths. The pressure was controlled by applying the Berendsen algorithm[50] with an isotropic pressure coupling, using a reference pressure of 1 atm, a relaxation time of 0.5 ps, and an isothermal compressibility of 4.5×10^{-5} bar^{-1}. Nonbonded interactions were calculated using a twin-range method with short- and long-range cutoffs of 8 and 14 Å,[51] respectively. A reaction field correction for electrostatic interactions was applied,[52,53] using dielectric constants of 78 and 67 for water and the ethanol/

dx.doi.org/10.1021/ci200455z | J. Chem. Inf. Model. 2012, 52, 465−473

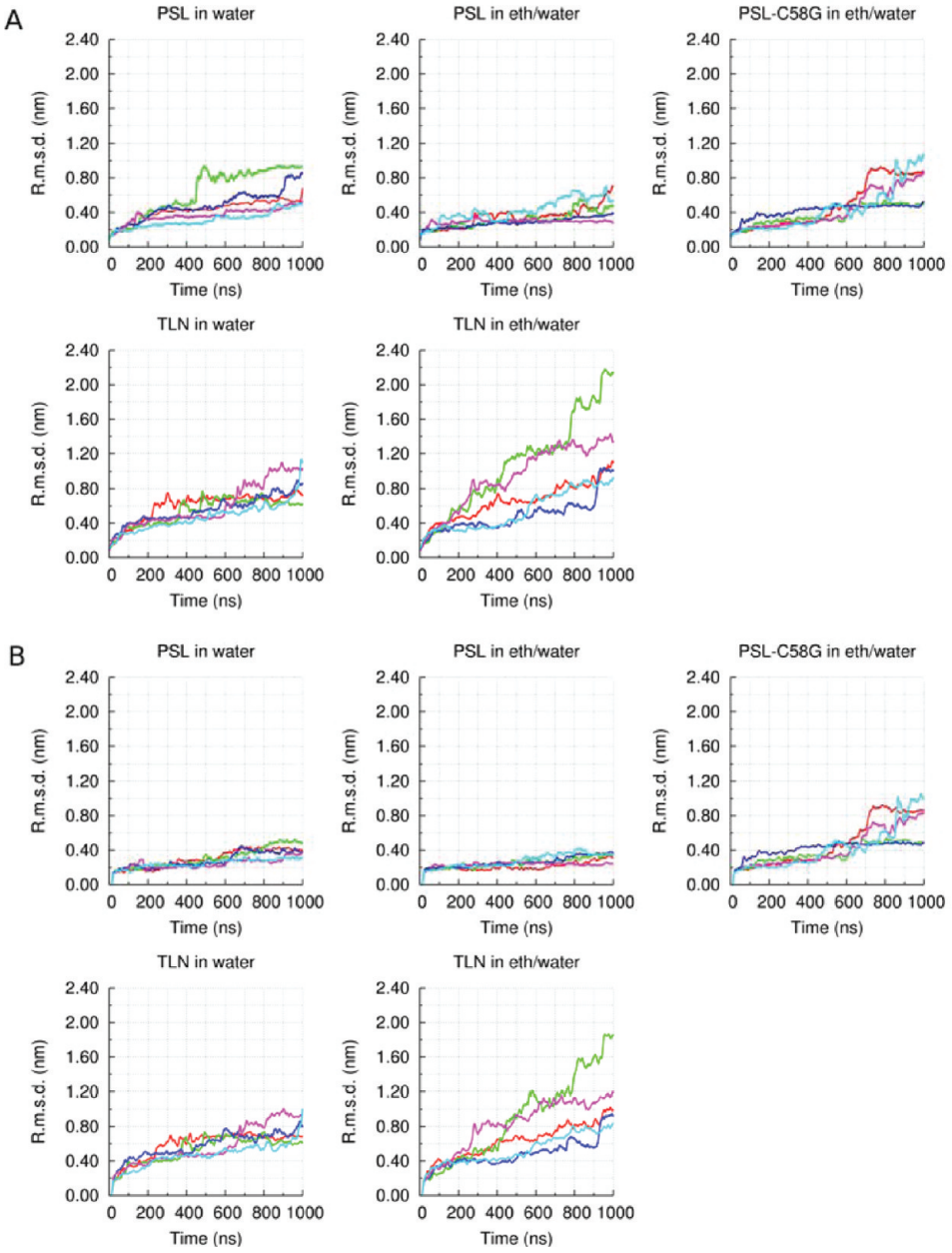

Figure 2. Moving average of the rmsd from the X-ray structure calculated using all the protein Cα atoms (panel A) and excluding the loop comprising residues 180−224 and 181−229 for PSL and TML, respectively (panel B). The different replicates are represented by lines with different colors (replicate 1: red, replicate 2: green, replicate 3: blue, replicate 4: magenta, and replicate 5: cyan).

water mixture (25% v/v), respectively.[54] The preparation of the systems to run the production MD simulations can be found in the Supporting Information.

RESULTS AND DISCUSSION

Structural Stability of the Proteins in Water and Ethanol/Water Simulations. A common way to analyze the structural stability of a protein in a MD simulation is to monitor the root-mean-square deviation (rmsd) from the initial structure along the simulation. The rmsd from of all the systems under study is shown in Figure 2A. It is clear from these plots that after 1 μs of simulation all the structures are considerably distinct from the X-ray structures that were employed as the starting point of the simulations. In the case of wild-type pseudolysin, the structure is more conserved in ethanol/water (average rmsd in the last 100 ns = 0.45 nm) than in the pure water simulations (average rmsd in the last 100 ns = 0.65 nm). This is in agreement with previous experimental findings that show that the half-life of pseudolysin in an ethanol/water solution (25% v/v) exceeds 100 days, whereas in aqueous solution it is around 9 days.[1] Studies of a closely related protease, elastase strain K, which has an identity of 99% with PSL, have also shown that this enzyme is more stable in ethanol/water mixtures (25% v/v) than in aqueous solution.[55] The pseudolysin mutant C58G in ethanol/water deviates more from the X-ray structure than the native enzyme (average rmsd in the last 100 ns = 0.72 nm), which is also in accordance with site-directed mutagenesis experiments, where it was found that the C58G mutant has a considerably lower half-life (~5 days)[2] than the wild-type.[2] Thermolysin is quite unstable in both media analyzed, although it clearly undergoes considerably

dx.doi.org/10.1021/ci200455z | J. Chem. Inf. Model. 2012, 52, 465−473

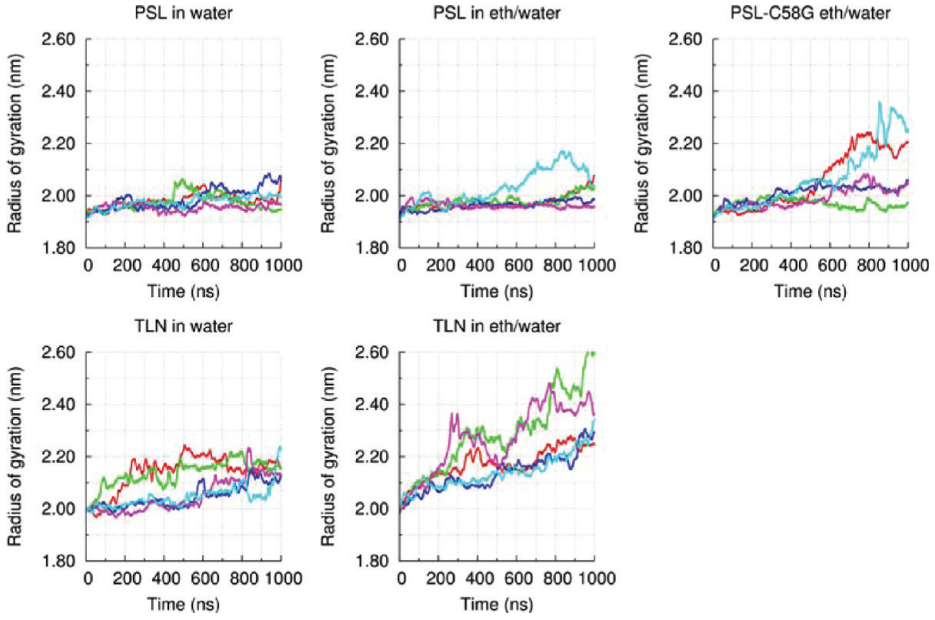

Figure 3. Moving average of the radius of gyration. The lines with different colors represent different replicates, as in Figure 2.

larger conformational changes in ethanol/water simulations than in pure water (the average rmsd values in the last 100 ns of simulation are 1.25 and 0.80 nm, for ethanol/water and water, respectively). Once again, this is consistent with the experimentally measured half-lives of TLN in ethanol/water and pure water, which are 3 and 10.8 days, respectively.[1] These results are also in line with another study, where it was observed that the thermal stability of thermolysin is severely decreased in the presence of 50% (v/v) of n-propanol, relative to aqueous solution.[56]

Visual inspection of the trajectories obtained in the simulations of pseudolysin gave us an indication that the largest conformational changes took place in the loop comprising residues 180−224 (highlighted in red in Figure 1), located in the C-terminal domain. Therefore, we performed new rmsd calculations without including this loop. Comparing the plots in Figure 2A,B, it can be seen that the rmsd of the wild-type pseudolysin is considerably lower when this loop is not included, especially in water simulations. This means that the high rmsd values observed in the wild-type pseudolysin simulations are mainly caused by the conformational changes in one of its loops and do not necessarily represent protein unfolding. In what concerns the pseudolysin mutant C58G, the rmsd obtained with or without including the loop is very similar, indicating that the structural changes are not localized in this loop and probably reflect global protein unfolding. In the simulations of thermolysin in water, the rmsd calculated without including the loop comprising residues 181−229 is very similar to the one obtained when the loop is included. In ethanol/water simulations, the rmsd of thermolysin is slightly lower when the loop is not included but remains higher than the one obtained in water.

Additionally, visual analysis led us to suspect that there were rigid body motions between the protein domains (especially in the case of TLN). This is in accordance with what has been previously observed in experimental and simulation studies,[57−59] where it was found that there is a hinge-bending motion between the N- and C-terminal domains of thermolysin. The structure obtained by Hausrath et al.[58] revealed that in the absence of a substrate, the enzyme adopts an open conformation which is not observed when the enzyme−ligand complex is formed. Although the TLN structure that was used in this study was obtained in the absence of inhibitors, it was subsequently found to have electron density in the active site that probably corresponds to a bound dipeptide which could be the result of autolysis during protein purification or crystallization,[59] suggesting that the closed conformation of the enzyme found in this structure is induced by the presence of the dipeptide, explaining why the protein opens during the simulations (where the peptide was not included). In order to investigate if there are rigid body motions between the protein domains, we calculated the rmsd of each domain separately (the results are shown and discussed in more detail in Supporting Information). This analysis shows that the rmsd values obtained for each separate domain of thermolysin are lower than the global rmsd, both in water and in ethanol/water simulations, which indicates that there are in fact rigid motions. In the case of pseudolysin, we only found significant interdomain movements in two replicates of the C58G mutant in ethanol/water.

Although the rmsd is a good measure of the degree of conservation of a structure, it is still limited, and other analyses, such as the radius of gyration and secondary structure content, can bring further insight. As can be observed in Figure 3, native PSL has approximately the same radius of gyration in pure water as in ethanol/water simulations (the average values in the last 100 ns of simulation are 1.99 and 2.02 nm for water and ethanol/water, respectively), whereas thermolysin is considerably more open in the ethanol/water mixture than in pure water (the average values in the last 100 ns of simulation are 2.14 and 2.35 nm for water and ethanol/water, respectively). The C58G mutant of pseudolysin is considerably less compact (average radius of gyration in the last 100 ns = 2.10 nm) than the wild-type enzyme in our ethanol/water simulations. The loss of compactness of TLN and the PSL mutant, in the ethanol/water mixture, indicates that these enzymes are unfolding. These results are consistent with our rmsd analysis and the previous experimental findings.[1]

dx.doi.org/10.1021/ci200455z | J. Chem. Inf. Model. 2012, 52, 465−473

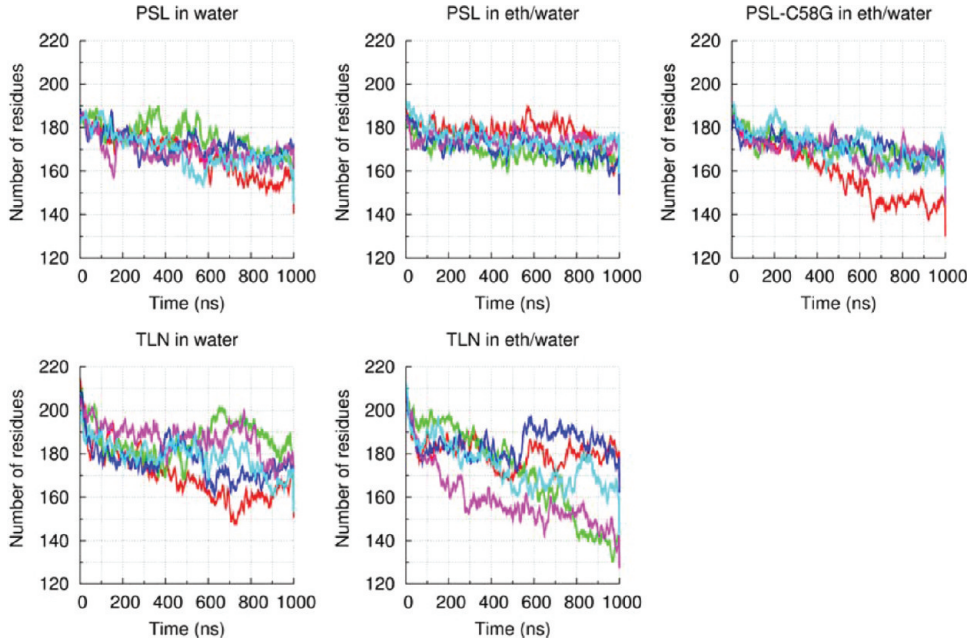

Figure 4. Moving average of the total secondary structure content computed as the sum of the number of residues that are part of α-helices, β-sheets, β-bridges, or turns, according to DSSP criterion.[61] The lines with different colors represent different replicates, as in Figure 2.

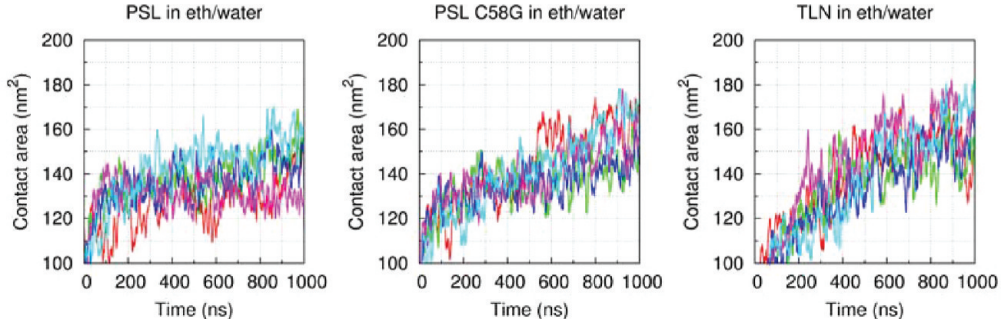

Figure 5. Moving average of the contact area between ethanol molecules and the protein. The protein−ethanol contact area is given by the following expression: $CA_{prot/eth} = SAS_{prot} + SAS_{eth} - SAS_{prot+eth}$, where $CA_{prot/eth}$ is the protein−ethanol contact area, SAS_{prot} is the solvent accessible surface of the protein, SAS_{eth} is the solvent accessible surface of ethanol, and $SAS_{prot+eth}$ is the solvent accessible surface of the protein−ethanol system. The lines with different colors represent different replicates, as in Figure 2.

The analysis of the secondary structure content of the proteins studied, in the two media used (Figure 4), indicates that the loss of secondary structure by pseudolysin is slightly more pronounced in water (average loss of secondary structure content ∼11%) than in ethanol/water simulations (average loss of secondary structure content ∼10%). Although our rmsd and radius of gyration analysis indicate that the mutant of pseudolysin is considerably more unstable than the wild-type enzyme in the ethanol/water mixture, this does not correspond to a clear difference in what concerns the loss of secondary structure, except in replicate 1 of the mutant, where there is a greater loss of secondary structure (note that this replicate is the one that has a higher rmsd, see Figure 2 and Figure S1, Supporting Information). There are two possible explanations for this fact: either the disulfide bridge plays a role in maintaining the enzyme tertiary structure but not its secondary structure or our sampling is not sufficient to distinguish between the two forms of the enzyme. The latter hypothesis is supported by the fact that in one of the mutant replicates we do observe a marked loss of secondary structure. Thermolysin suffers a higher loss of secondary structure content in ethanol/water (average loss of secondary structure content ∼21%) than in pure water simulations (average loss of secondary structure content ∼16%), which is consistent with the results discussed above. Our secondary structure analysis is in line with a previous study, in which the authors determined the CD spectra of PSL and TLN in the presence and in the absence of methanol, and found that the secondary structure of pseudolysin was more conserved in the presence of methanol, whereas the opposite was observed for thermolysin.[60]

Protein−Ethanol Interaction. With the aim of understanding the molecular determinants underlying the stability of PSL (wild-type and C58G mutant) and TML in media containing ethanol, we analyzed the contact area between the enzymes and the alcohol. Figure 5 shows that the protein−ethanol contact area reaches higher values at the end of the simulation in the C58G mutant of pseudolysin than in the wild-type (157 vs 147 nm^2 for the mutant and wild-type, respectively), and in the mutant, it is still increasing after 1 μs of simulation, whereas the native pseudolysin/ethanol contact area appears to reach a plateau after the first 200 ns of simulation. These results indicate that the mutant PSL has a

dx.doi.org/10.1021/ci200455z | J. Chem. Inf. Model. 2012, 52, 465−473

greater tendency to interact with ethanol than the wild-type enzyme. As can be seen in Figure 5, thermolysin has a strong propensity to interact with ethanol molecules, given that the contact area between this protein and ethanol increases sharply in the first 500 ns of simulation (reaching a value of 159.51 nm^2 in the last 100 ns of simulation).

As a control we also measured the contact area between the protein and the water. Figure S2, Supporting Information, shows that the wild-type and mutant pseudolysin have similar contact areas with water (average values of 190.16 and 191.03 nm^2 for the wild-type and mutant, respectively). The contact area between thermolysin and water is larger than in the case of pseudolysin (average value of 215.59 nm^2), which is not surprising, given that TLN has a larger solvent accessible surface than PSL.

To complete our analysis of the interaction between the proteins under study and ethanol, we investigated if this interaction is mainly polar or hydrophobic. The distribution of ethanol molecules around the protein surface is displayed in Figure 6. In this plot, there are two clearly distinct peaks, the

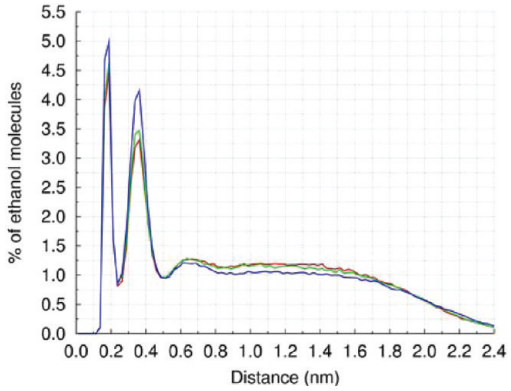

Figure 6. Distribution of the ethanol molecules around the protein in the last 100 ns of the simulations performed in the ethanol/water mixture. The red, green, and blue lines correspond to wt PSL, mutant C58G of PSL, and TLN, respectively.

first one is centered at ~0.2 nm and corresponds to ethanol molecules that form hydrogen bonds with the protein, and the second one is centered at ~0.35 nm and corresponds to van der Waals interactions between ethanol molecules and the protein. The area of the second peak is larger than the area of the first peak for the three proteins analyzed (see Table S1, Supporting Information), meaning that the majority of the interactions between the protein and the ethanol are van der Waals interactions. Comparing the areas of the peaks of the three proteins (Table S1, Supporting Information), we can see that thermolysin has a higher number of interactions (which are mainly hydrophobic) with ethanol than pseudolysin. The peaks of the mutant pseudolysin are slightly larger than the peaks of the wild-type enzyme (especially the second peak), meaning that the mutant has a higher number of hydrophobic interactions with ethanol, which is in agreement with the results obtained in the analysis of the protein−ethanol contact surface (see above). As a control, we analyzed the distribution of water molecules around the proteins. Figure S3 and Table S2, Supporting Information, show that the distribution of water molecules is very similar for the three proteins, in the simulations performed in ethanol/water mixtures.

To further elucidate the nature of the interactions between the protein and the ethanol, we analyzed the distributions of the alcohol (OH) and alkyl (CH_2CH_3) moieties of the molecule, separately. In Figure S4A, Supporting Information, we can see that the OH group interacts with the protein through hydrogen bonding (first peak) and van der Waals interactions (second peak). The areas of the two peaks (Table S3, Supporting Information) indicate that the former is the predominant type of interaction for all the proteins analyzed. Both moieties of the ethanol molecule have a peak centered at ~0.35 nm that corresponds to van der Waals interactions with the protein. This means that both moieties contribute to the second peak observed in Figure 6, although the contribution of alkyl moiety is larger than that of the alcohol moiety.

The observation that thermolysin tends to form hydrophobic interactions with alcohol molecules is in agreement with a previous crystallographic analysis, in which thermolysin crystals were soaked with isopropanol. In that study, 12 different binding sites for isopropanol were identified, and most of these binding sites were located in hydrophobic pockets.[62] Interestingly, 10 of the 12 isopropanol crystallographic binding sites correspond to residues which interact very frequently with ethanol molecules in our simulations (see Figure S5, Supporting Information). The remaining two binding sites found in the X-ray structure are formed by more than one molecule in the crystal lattice, and therefore it is not surprising that they are not very populated during the simulations. The agreement between our results and the experimental findings is a very good indicator that our observations are realistic. Our results are also in line with a biochemical study where it was observed that more hydrophobic solvents cause a more severe decrease in the thermal stability of thermolysin than more hydrophilic ones,[56] which indicates that the solvent destabilizes the enzyme because it can bind to hydrophobic pockets and distort its tertiary structure. Additionally, another study has shown that there is a negative correlation between the polarity index of a solvent and its power to irreversibly denature enzymes,[63] which is most likely due to the fact that apolar solvents can bind to hydrophobic regions of the proteins and lead to their irreversible unfolding.

Comparing the Behavior of Wild-Type and C58G Mutant of Pseudolysin. One of the aims of this work is to elucidate the role played by the disulfide bridge between C30 and C58 in maintaining the stability of pseudolysin in ethanol/water mixtures. Toward this end, we compared the behavior of the wild-type and the C58G mutant of pseudolysin in the simulations performed in the ethanol/water mixture. In order to analyze the major conformational changes that occur during the simulations, we divided each trajectory in 10 ns windows and calculated the average structure in each window. The results are displayed in movies S1 and S2 (see Supporting Information). These movies show that, in agreement with the results discussed above, the mutant enzyme suffers larger conformational changes than the wild-type. Focusing on the region where the residues C30 and (C/G)58 are located (highlighted in magenta), we can see that these loops undergo larger conformational changes in the mutant than in the wild-type simulations, indicating that the disulfide bridge constrains the motion of these loops. In the absence of this bond, the loops are free to move and consequently become more unstable. Nevertheless, it is clear from movie S2 (see Supporting Information) that the large conformational changes of the C58G mutant of pseudolysin are not restricted to these

dx.doi.org/10.1021/ci200455z | J. Chem. Inf. Model. 2012, 52, 465−473

loops. One example of this is the behavior of replicate 1, where we can observe large conformational changes in the C-terminal domain (located in the opposite side of the protein). Analyzing the distribution of ethanol around the enzyme in this simulation (see movie S3, Supporting Information) we can see that after about 500 ns of simulation, ethanol starts to accumulate in the interior of the protein, surrounding the α-helices located in the C-terminal domain, and at the same time, this region of the enzyme starts to unfold until it gets completely destroyed. These observations indicate that in the absence of the disulfide bridge between the loops, they become more flexible. It is possible that the conformational changes of the loops are then propagated to other regions of the enzyme, which can become more open and, therefore, more permeable to ethanol molecules. The accumulation of ethanol in these regions will substitute essential intraprotein hydrophobic interactions, leading to unfolding.

CONCLUDING REMARKS

Using a MD simulation approach, we were able to obtain a molecular picture that explains the experimentally observed difference in stability of pseudolysin and thermolysin in ethanol/water solutions. In accordance with the previous experimental findings,[1] pseudolysin is more stable than thermolysin in the simulations performed in ethanol/water media. The analysis of the interaction between the proteins and ethanol showed that the contact surface between thermolysin and the alcohol is larger than that of pseudolysin. Our results also indicate that the nature of the interaction between the proteins and ethanol is mainly hydrophobic, and therefore, the alcohol molecules that reach the interior of thermolysin will replace the native intraprotein hydrophobic interactions, leading to the unfolding of the enzyme.

We also found that, in agreement with site-directed mutagenesis experiments,[2] the absence of the C30−C58 disulfide bond makes pseudolysin more unstable. The investigation of the protein−ethanol interaction showed that the mutant C58G has a larger protein−ethanol contact surface than the wild-type enzyme. Our results indicate that the disulfide bridge constrains the motion of the loops that it connects. In the mutant (which lacks this bridge) the loops undergo higher conformational changes than in the wild-type. We think that these conformational changes can propagate to other regions of the enzyme, causing it to open and enabling ethanol molecules to penetrate. Analogously to what happens in the case of thermolysin, these ethanol molecules can disrupt essential intraprotein interactions, which explains the low stability of the mutant in ethanol/water mixtures.

The results presented here are in good agreement with several experimental studies, which shows that simulation studies can mimic what is observed experimentally concerning the stability of enzymes in solutions containing organic solvents. Additionally, this study complements the previous experimental works by providing a molecular explanation for their observations and may be used in the prediction and engineering of optimized enzymes for this type of media.

ASSOCIATED CONTENT

Supporting Information

Protocols used to prepare the systems for the production and MD simulations and to determine the protonation states of the ionizable residues of the protein. Analysis of rigid body motions between the protein domains. Plot of the distribution of the alcohol (OH) and alkyl (CH_2CH_3) moieties of the ethanol molecule around the protein. Plot of the distribution of the water molecules around the protein. Tables with the areas of the peaks of the histograms. Movies showing the behavior of the mutant and wild-type pseudolysin and the distribution probability density of ethanol in replicate 1 of the C58G mutant of pseudolysin. This information is available free of charge via the Internet at http://pubs.acs.org.

AUTHOR INFORMATION

Corresponding Author

*E-mail: claudio@itqb.unl.pt. Telephone: +351214469610.

Notes

The authors declare no competing financial interest.

ACKNOWLEDGMENTS

The authors acknowledge Dr. Nuno Micaêlo, Prof. Susana Barreiros and Prof. André Melo for helpful discussions, and the financial support from Fundação para a Ciência e a Tecnologia, Portugal, through grants SFRH/BD/28269/2006, POCTI/BIO/57193/2004 and PEst-OE/EQB/LA0004/2011.

REFERENCES

(1) Ogino, H.; Watanabe, F.; Yamada, M.; Nakagawa, S.; Hirose, T.; Noguchi, A.; Yasuda, M.; Ishikawa, H. Purification and characterization of organic solvent-stable protease from organic solvent-tolerant Pseudomonas aeruginosa PST-01. *J. Biosci. Bioeng.* **1999**, *87*, 61−68.

(2) Ogino, H.; Uchiho, T.; Yokoo, J.; Kobayashi, R.; Ichise, R.; Ishikawa, H. Role of intermolecular disulfide bonds of the organic solvent-stable PST-01 protease in its organic solvent stability. *Appl. Env. Microb.* **2001**, *67*, 942−947.

(3) Klibanov, A. M. Improving enzymes by using them in organic solvents. *Nature* **2001**, *409*, 241−245.

(4) Zaks, A.; Klibanov, A. M. Enzyme-catalyzed processes in organic solvents. *Proc. Natl. Acad. Sci. U.S.A.* **1985**, *82*, 3192−3196.

(5) Zaks, A.; Klibanov, A. M. Substrate-specificity of enzymes in organic-solvents vs. water is reversed. *J. Am. Chem. Soc.* **1986**, *108*, 2767−2768.

(6) Secundo, F.; Riva, S.; Carrea, G. Effects of medium and of reaction conditions on the enantioselectivity of lipases in organic-solvents and possible rationales. *Tetrahedron: Asymmetry* **1992**, *3*, 267−280.

(7) Nakamura, K.; Takebe, Y.; Kitayama, T.; Ohno, A. Effect of solvent structure of enantioselectivity on lipase-catalyzed trans-esterification. *Tetrahedron Lett.* **1991**, *32*, 4941−4944.

(8) Fitzpatrick, P. A.; Klibanov, A. M. How can the solvent affect enzyme enantioselectivity? *J. Am. Chem. Soc.* **1991**, *113*, 3166−3171.

(9) Micaelo, N. M.; Teixeira, V. H.; Baptista, A. M.; Soares, C. M. Water dependent properties of cutinase in nonaqueous solvents: A computational study of enantioselectivity. *Biophys. J.* **2005**, *89*, 999−1008.

(10) Klibanov, A. M. Enzyme memory - What is remembered and why. *Nature* **1995**, *374*, 596−596.

(11) Russell, A. J.; Klibanov, A. M. Inhibitor-induced enzyme activation in organic-solvents. *J. Biol. Chem.* **1988**, *263*, 11624−11626.

(12) Staahl, M.; Jeppsson-Wistrand, U.; Maansson, M. O.; Mosbach, K. Induced stereo- and substrate selectivity of bioimprinted alpha-chymotrypsin in anhydrous organic media. *J. Am. Chem. Soc.* **1991**, *113*, 9366−9368.

(13) Lousa, D.; Baptista, A. M.; Soares, C. M. Structural determinants of ligand imprinting: A molecular dynamics simulation study of subtilisin in aqueous and apolar solvents. *Protein Sci.* **2011**, *20*, 379−386.

(14) Bevc, S.; Konc, J.; Stojan, J.; Hodoscek, M.; Penca, M.; Praprotnik, M.; Janezic, D. ENZO: A Web Tool for Derivation and

Evaluation of Kinetic Models of Enzyme Catalyzed Reactions. *PLoS One* **2011**, *6*, e22265.
(15) Johnson, K. A. Fitting Enzyme Kinetic Data with Kintek Global Kinetic Explorer. *Meth. Enzymol.* **2009**, *467*, 601−626.
(16) Kuzmic, P. DynaFit - A Software Package for Enzymology. *Meth. Enzymol.* **2009**, *467*, 247−280.
(17) Walsh, R.; Martin, E.; Darvesh, S. A method to describe enzyme-catalyzed reactions by combining steady state and time course enzyme kinetic parameters. *Biochim. Biophys. Acta, Gen. Subj.* **2010**, *1800*, 1−5.
(18) Soares, C. M.; Teixeira, V. H.; Baptista, A. M. Protein structure and dynamics in nonaqueous solvents: Insights from molecular dynamics simulation studies. *Biophys. J.* **2003**, *84*, 1628−1641.
(19) Micaelo, N. M.; Soares, C. M. Modeling hydration mechanisms of enzymes in nonpolar and polar organic solvents. *FEBS J.* **2007**, *274*, 2424−2436.
(20) Micaelo, N. M.; Soares, C. M. Protein structure and dynamics in ionic liquids. Insights from molecular dynamics simulation studies. *J. Phys. Chem. B* **2008**, *112*, 2566−2572.
(21) Cruz, A.; Ramirez, E.; Santana, A.; Barletta, G.; Lopez, G. E. Molecular dynamic study of subtilisin Carlsberg in aqueous and nonaqueous solvents. *Mol. Simul.* **2009**, *35*, 205−212.
(22) Trodler, P.; Schmid, R. D.; Pleiss, J. Modeling of solvent-dependent conformational transitions in Burkholderia cepacia lipase. *BMC Struct. Biol.* **2009**, *9*, 38−50.
(23) Benkovic, S. J.; Hammes, G. G.; Hammes-Schiffer, S. Free-energy landscape of enzyme catalysis. *Biochemistry* **2008**, *47*, 3317−3321.
(24) Kamerlin, S. C. L.; Warshel, A. The EVB as a quantitative tool for formulating simulations and analyzing biological and chemical reactions. *Faraday Discuss.* **2010**, *145*, 71−106.
(25) McGeagh, J. D.; Ranaghan, K. E.; Mulholland, A. J. Protein dynamics and enzyme catalysis: Insights from simulations. *Biochim. Biophys. Acta, Proteins Proteomics* **2011**, *1814*, 1077−1092.
(26) Acevedo, O.; Jorgensen, W. L. Advances in Quantum and Molecular Mechanical (QM/MM) Simulations for Organic and Enzymatic Reactions. *Acc. Chem. Res.* **2010**, *43*, 142−151.
(27) Roccatano, D. Computer simulations study of biomolecules in non-aqueous or cosolvent/water mixture solutions. *Curr. Protein Pept. Sci.* **2008**, *9*, 407−426.
(28) Hudson, E. P.; Eppler, R. K.; Clark, D. S. Biocatalysis in semi-aqueous and nearly anhydrous conditions. *Curr. Opin. Biotechnol.* **2005**, *16*, 637−643.
(29) Gupta, M. N.; Roy, I. Enzymes in organic media - Forms, functions and applications. *Eur. J. Biochem.* **2004**, *271*, 2575−2583.
(30) Iyer, P. V.; Ananthanarayan, L. Enzyme stability and stabilization - Aqueous and non-aqueous environment. *Proc. Biochem.* **2008**, *43*, 1019−1032.
(31) Gupta, A.; Khare, S. K. Enzymes from solvent-tolerant microbes: Useful biocatalysts for non-aqueous enzymology. *Crit. Rev. Biotechnol.* **2009**, *29*, 44−54.
(32) Doukyu, N.; Ogino, H. Organic solvent-tolerant enzymes. *Biochem. Eng. J.* **2010**, *48*, 270−282.
(33) Jensen, S. E.; Fecycz, I. T.; Campbell, J. N. Nutritional factors controlling exocellular protease production by *Pseudomonas aeruginosa*. *J. Bacteriol.* **1980**, *144*, 844−847.
(34) Morihara, K.; Tsuzuki, H.; Oda, K. Protease and Elastase of *Pseudomonas aeruginosa* - Inactivation of Human-Plasma Alpha-1-Proteinase Inhibitor. *Infect. Immun.* **1979**, *24*, 188−193.
(35) Pavlovskis, O. R.; Wretlind, B. Assessment of protease (elastase) as a *Pseudomonas aeruginosa* virulence factor in experimental mouse burn infection. *Infect. Immun.* **1979**, *24*, 181−187.
(36) Morihara, K. Production of elastase and proteinase by *Pseudomonas aeruginosa*. *J. Bacteriol.* **1964**, *88*, 745−757.
(37) Heck, L. W.; Morihara, K.; Mcrae, W. B.; Miller, E. J. Specific cleavage of human type-III and IV collagens by *Pseudomonas aeruginosa* elastase. *Infect. Immun.* **1986**, *51*, 115−118.
(38) Holder, I. A.; Wheeler, R. Experimental studies of the pathogenesis of infections owing to *Pseudomonas aeruginosa*: elastase, an Igg Protease. *Can. J. Microbiol.* **1984**, *30*, 1118−1124.
(39) Matsubara, H.; Sasaki, R.; Singer, A.; Jukes, T. H. Specific nature of hydrolysis of insulin and tobacco mosaic virus protein by thermolysin. *Arch. Biochem. Biophys.* **1966**, *115*, 324−331.
(40) Holland, D. R.; Hausrath, A. C.; Juers, D.; Matthews, B. W. Structural analysis of zinc substitutions in the active site of thermolysin. *Protein Sci.* **1995**, *4*, 1955−1965.
(41) Thayer, M. M.; Flaherty, K. M.; Mckay, D. B. 3-Dimensional structure of the elastase of Pseudomonas aeruginosa at 1.5 A resolution. *J. Biol. Chem.* **1991**, *266*, 2864−2871.
(42) Baptista, A. M.; Soares, C. M. Some theoretical and computational aspects of the inclusion of proton isomerism in the protonation equilibrium of proteins. *J. Phys. Chem. B* **2001**, *105*, 293−309.
(43) Baptista, A. M.; Martel, P. J.; Soares, C. M. Simulation of electron-proton coupling with a Monte Carlo method: Application to cytochrome c3 using continuum electrostatics. *Biophys. J.* **1999**, *76*, 2978−2998.
(44) Berendsen, H. J. C.; van der Spoel, D.; van Drunen, R. GROMACS: A message-passing parallel molecular-dynamics implementation. *Comput. Phys. Commun.* **1995**, *91*, 43−56.
(45) Hess, B.; Kutzner, C.; van der Spoel, D.; Lindahl, E. GROMACS 4: Algorithms for highly efficient, load-balanced, and scalable molecular simulation. *J. Chem. Theory Comput.* **2008**, *4*, 435−447.
(46) Oostenbrink, C.; Villa, A.; Mark, A. E.; Van Gunsteren, W. F. A biomolecular force field based on the free enthalpy of hydration and solvation: The GROMOS force-field parameter sets 53A5 and 53A6. *J. Comput. Chem.* **2004**, *25*, 1656−1676.
(47) Hermans, J.; Berendsen, H. J. C.; van Gunsteren, W. F.; Postma, J. P. M A consistent empirical potential for water-protein interactions. *Biopolymers* **1984**, *23*, 1513−1518.
(48) Hess, B.; Bekker, H.; Berendsen, H. J. C.; Fraaije, J. G. E. M. LINCS: A linear constraint solver for molecular simulations. *J. Comput. Chem.* **1997**, *18*, 1463−1472.
(49) Miyamoto, S.; Kollman, P. A. SETTLE: an analytical version of the SHAKE and RATTLE algorithm for rigid water models. *J. Comput. Chem.* **1992**, *13*, 952−962.
(50) Berendsen, H. J. C.; Postma, J. P. M; van Gunsteren, W. F.; Dinola, A.; Haak, J. R. Molecular-dynamics with coupling to an external bath. *J. Chem. Phys.* **1984**, *81*, 3684−3690.
(51) van Gunsteren, W. F.; Berendsen, H. J. C. Computer simulation of molecular dynamics: Methodology, applications, and perspectives in chemistry. *Angew. Chem., Int. Ed.* **1990**, *29*, 992−1023.
(52) Barker, J. A.; Watts, R. O. Monte-Carlo studies of dielectric properties of water-like models. *Mol. Phys.* **1973**, *26*, 789−792.
(53) Tironi, I. G.; Sperb, R.; Smith, P. E.; van Gunsteren, W. F. A generalized reaction field method for molecular-dynamics simulations. *J. Chem. Phys.* **1995**, *102*, 5451−5459.
(54) Akerlof, G. Dielectric constants of some organic solvent-water mixtures at various temperatures. *J. Am. Chem. Soc.* **1932**, *54*, 4125−4139.
(55) Rahman, R. N. Z. R. A.; Salleh, A.; Basri, M.; Wong, C. F. Role of alpha-helical structure in organic solvent-activated homodimer of elastase strain K. *Int. J. Mol. Sci.* **2011**, *12*, 5797−5814.
(56) Pazhang, M.; Khajeh, K.; Ranjbar, B.; Hosseinkhani, S. Effects of water-miscible solvents and polyhydroxy compounds on the structure and enzymatic activity of thermolysin. *J. Biotechnol.* **2006**, *127*, 45−53.
(57) van Aalten, D. M. F.; Amadei, A.; Linssen, A. B. M.; V.G.H., E.; Vriend, G.; Berendsen, H. J. C. The essential dynamics of thermolysin: Confirmation of the hinge-bending motion and comparison of simulations in vacuum and water. *Proteins: Struct., Funct., Genet.* **1995**, *22*, 45−54.
(58) Hausrath, A. C.; Matthews, B. W. Thermolysin in the absence of substrate has an open conformation. *Acta Crystallogr., Sect. D: Biol. Crystallogr.* **2002**, *58*, 1002−1007.
(59) Holland, D. R.; Tronrud, D. E.; Pley, H. W.; Flaherty, K. M.; Stark, W.; Jansonius, J. N.; Mckay, D. B.; Matthews, B. W. Structural

comparison suggests that thermolysin and related neutral proteases undergo hinge-bending motion during catalysis. *Biochem.* **1992**, *31*, 11310−11316.
(60) Ogino, H.; Gemba, Y.; Yutori, Y.; Doukyu, N.; Ishimi, K.; Ishikawa, H. Stabilities and conformational transitions of various proteases in the presence of an organic solvent. *Biotechnol. Prog.* **2007**, *23*, 155−161.
(61) Kabsch, W.; Sander, C. Dictionary of protein secondary structure - Pattern-recognition of hydrogen-bonded and geometrical features. *Biopolymers* **1983**, *22*, 2577−2637.
(62) English, A. C.; Done, S. H.; Caves, L. S. D.; Groom, C. R.; Hubbard, R. E. Locating interaction sites on proteins: The crystal structure of thermolysin soaked in 2% to 100% isopropanol. *Proteins: Struct., Funct., Genet.* **1999**, *37*, 628−640.
(63) Gupta, M. N.; Batra, R.; Tyagi, R.; Sharma, A. Polarity index: The guiding solvent parameter for enzyme stability in aqueous-organic cosolvent mixtures. *Biotechnol. Prog.* **1997**, *13*, 284−288.